

**ASSESSING THE ROLE OF TRANSPORT MECHANISMS
AND MODEL PARAMETERS ON CONTAMINANT PLUME
DYNAMICS AND HEALTH RISK METRICS FOR THE
SUBSURFACE ENVIRONMENT**

ABHAY



**DEPARTMENT OF CIVIL ENGINEERING
INDIAN INSTITUTE OF TECHNOLOGY DELHI**

JULY 2024

© Indian Institute of Technology Delhi (IITD), New Delhi, 2024

**ASSESSING THE ROLE OF TRANSPORT MECHANISMS
AND MODEL PARAMETERS ON CONTAMINANT PLUME
DYNAMICS AND HEALTH RISK METRICS FOR THE
SUBSURFACE ENVIRONMENT**

by

ABHAY

Department of Civil Engineering

Submitted

in fulfillment of the requirements of the degree of **DOCTOR OF PHILOSOPHY**

to the



INDIAN INSTITUTE OF TECHNOLOGY DELHI

JULY 2024

*This thesis is dedicated to my beloved parents and my sister
for their endless love, support, and encouragement....*

and

*to those who are knowingly or unknowingly exposed to
waste-contaminated sites.*

CERTIFICATE

This is to certify that the thesis entitled “**Assessing the Role of Transport Mechanisms and Model Parameters on Contaminant Plume Dynamics and Health Risk Metrics for the Subsurface Environment**” submitted by **Abhay** to the Indian Institute of Technology Delhi for the award of the degree of **Doctor of Philosophy** is a bona fide record of research work carried out by him under my supervision. In my opinion, the thesis work has reached the requisite standards, fulfilling the requirements for the degree of Doctor of Philosophy.

The contents of this thesis, in full or in parts, have not been submitted to any other University or Institute for the award of any other degree or diploma.

Prof. Sumedha Chakma

Associate Professor, Department of Civil Engineering

Indian Institute of Technology Delhi

Hauz Khas, New Delhi-110016

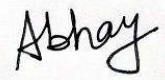
ACKNOWLEDGEMENTS

I am using this opportunity to express my gratitude to my supervisor, Prof. Sumedha Chakma, who has supported me throughout my research work. I am thankful for his aspiring guidance, invaluable constructive criticism, and friendly advice during the research work. I am sincerely grateful to him for sharing his truthful and illuminating views on several issues related to the thesis.

My sincere thanks to my research committee members, Prof. Vasant A. Matsagar, Prof. B.R. Chahar, and Prof. Gaurav Goel, for their valuable suggestions on my research. I would like to express thanks for the collaborative work with Dr. Pankaj Kumar Gupta (Ramanujan Fellow, IIT Delhi), Prof. Brijesh Kumar Yadav (Dept. of Hydrology, IIT Roorkee), and Dr Rahul Singh (IIT Delhi). I also want to thank unknown reviewers for their valuable comments, which significantly improved the quality of work and manuscripts of published journal articles. I would also like to sincerely thank Mr N.R. Gehlot (Simulation Lab, Civil Engineering Department) and Mr. Saran for their help in workstation-related queries.

Most importantly, I express my warm thanks to all my friends, especially Sudeep V. Banad, Umesh Sharma, Dr. Sharad (UFZ Leipzig, Germany) and Naman (IIT Kharagpur), Ravi Raj, Priyam Deka, Rajat, Nirdesh Sharma, Saarthi Sharma, and Devavat Chiru Naik, and fellow research group mates (Dipto Deb, Maliha Ashraf, Kamalakanta Sahu, Nekita Boraah, Roohmoney, and Caleb White) for their companionship, support, and encouragement during the tenure of this work. I want to thank my colleagues (Durga Prasad Tripathi, Aasif, Ashish Dobhal, and Mohd. Aman Khalid) for all the discussion and fun during the coursework.

I would like to express my greatest gratitude to my beloved mother, Smt. Bhawna Guleria, for her endless and unconditional support and love, my father, Sh. Lajpat Guleria and my sister, Kamna, for their constant love and encouragement. Without them, this journey could never be accomplished. I would like to thank all those people, friends, and relatives who have directly and indirectly helped me throughout this journey. Above all, I am thankful to the Almighty for his/her divine blessings and for giving me the required courage and strength during difficult times.

A handwritten signature in black ink that reads "Abhay". The signature is written in a cursive style with a capital 'A' and a lowercase 'bhay'.

ABSTRACT

Groundwater contamination is increasingly challenging and impacting the ecological environment and human health. To design remediation operations for contaminated regions, contaminant transport models that incorporate uncertainty associated with fate and transport mechanisms need to be developed. Health risk models are necessary to effectively transfer knowledge from technical to non-technical audiences. Moreover, health risk models should include the uncertainty associated with exposure model parameters, site- and activity-specific scenarios and exposure pathways for effective risk communication. This research delves into a multifaceted investigation of contaminant transport in the presence of low permeability porous media (LPPM) and dead-end regions and health risk assessment of the subsurface environment. A probabilistic human health risk assessment (HHRA) framework considering uncertainty in exposure model parameters such as body weight (BW), ingestion rate (IR), exposure frequency (EF), exposure duration (ED), skin surface area (SA) was developed to estimate non-carcinogenic hazard quotient (HQ) due to metal leaching from dumping sites (Okhla, Ghazipur, and Bhalswa landfill sites of Delhi, Ariyamangalam, and fly-ash dumping site Nasik) in India. Fly-ash dumping site in Nasik was found to pose the highest risk to human health in comparison to remaining considered dumping sites. An enormous difference between estimated HQ (child) and HQ (adult) for both the oral ingestion and skin dermal exposure scenarios was not observed. The variance attribution analysis indicated that the BW and ED contributed 35% to 55% towards the overall uncertainties of estimated HQs for children, and more than 95% of the contribution for adults was found to be governed by ED. An integrated ecological and HHRA framework was developed to assess the ecological and human health risks due to chromite ore processing residue (COPR) dumpsites in

Kanpur, India. The multiple exposure scenarios (oral ingestion and skin dermal contact) and multiple pathways (soil and groundwater pathways) along the activity-specific scenarios were considered in the risk assessment framework. The teen playing in mud activity was found in the highest risk zone among all exposure scenarios in all population groups. The average value of HQ was found to be 4.5, which is four orders higher than the safe limit, and the 95th percentile value of cancer risk (CR) was found to be 9×10^{-4} for skin dermal contact exposure scenario via soil pathway. The presence of Cr(VI) and U in groundwater near the Rania site, above the safe limit, was found to pose a significant threat to every population group. The maximum value of CR was found to be 54.9, the highest among all population groups.

A novel Teaching Learning-based Optimization (TLBO) and mobile-immobile (MIM) model-based integrated approach was implemented to simulate the solute transport through heterogeneous short- (30 cm) and long-column (12.5 m) conditions. The MIM model was found to capture the early arrival of solute, peak concentration, and long tailing in the breakthrough curve (BTC) well for conservative solute transport in 12.5 m long highly heterogeneous soil column and reactive solute transport in a 30 cm column-filled with Glendale clay loam soil. Further, the uncertainty associated with flow and transport parameters of multispecies contaminants was quantified using Global Sensitivity Analysis (GSA). GSA of contaminant transport model based on temporal moment-based output indices indicated the complex interplay between different model parameters and their varying influences on different output indices. This research discussed the contrasting plume evolution dynamics observed in porous systems with and without LPPM regions from two-dimensional (2-D) numerical simulations. The contaminant mass recovery and mean residence time were found to be 25% to 50% lower and 25% to 40% higher in the porous system with the LPPM region than in the porous system without it, respectively. In the end,

contaminant transport model-driven probabilistic HHRA was conducted for a chemical mixture of Tetrachloroethene (also known as PCE) and its transformation products. The transformed daughter species i.e., Vinyl Chloride (VC), and cis-Dichloroethene (cis-DCE) were found to pose the highest risk to human health for a longer duration (up to 15 years) than the parent contaminant species i.e., PCE. The BW, concentration, ED, and IR were found to be major contributors to the total variance in the estimated risk metrics. Overall, the probabilistic risk assessment approaches, and numerical methods to analyze contaminant plume dynamics introduced in this thesis can be helpful in understanding the complexities involved in fate and contaminant transport and for policymakers to transfer knowledge from technical to non-technical audiences effectively.

सार

भूजल प्रदूषण तेजी से चुनौतीपूर्ण हो रहा है और पारिस्थितिक पर्यावरण और मानव स्वास्थ्य पर प्रभाव डाल रहा है। दूषित क्षेत्रों के लिए उपचारात्मक कार्यों को डिजाइन करने के लिए, दूषित परिवहन मॉडल विकसित करने की आवश्यकता है जिसमें भाग्य और परिवहन तंत्र से जुड़ी अनिश्चितता शामिल हो। तकनीकी से गैर-तकनीकी दर्शकों तक ज्ञान को प्रभावी ढंग से स्थानांतरित करने के लिए स्वास्थ्य जोखिम मॉडल आवश्यक हैं। इसके अलावा, स्वास्थ्य जोखिम मॉडल में एक्सपोज़र मॉडल मापदंडों, स्थल और गतिविधि विशिष्ट परिदृश्यों और प्रभावी जोखिम संचार के लिए एक्सपोज़र मार्गों से जुड़ी अनिश्चितता शामिल होनी चाहिए। यह शोध कम पारगम्यता वाले झरझरा मीडिया (एलपीपीएम [LPPM]) और मृत-अंत क्षेत्रों की उपस्थिति में दूषित परिवहन की बहुमुखी जांच और उपसतह पर्यावरण के स्वास्थ्य जोखिम मूल्यांकन पर प्रकाश डालता है। शरीर के वजन (बीडब्ल्यू [BW]), अंतर्ग्रहण दर (आईआर [IR]), एक्सपोज़र आवृत्ति (ईएफ [EF]), एक्सपोज़र अवधि (ईडी [ED]), त्वचा की सतह क्षेत्र (एसए [SA]) जैसे एक्सपोज़र मॉडल मापदंडों में अनिश्चितता पर विचार करते हुए एक संभाव्य मानव स्वास्थ्य जोखिम मूल्यांकन (एचएचआरए [HHRA]) ढांचा विकसित किया गया था भारत में डंपिंग साइटों (दिल्ली के ओखला, गाज़ीपुर, और भलस्वा लैंडफिल साइट, अरियामंगलम और फ्लार्ड-ऐश डंपिंग साइट नासिक) से धातु की लीचिंग के कारण गैर-कैंसरजन्य खतरे के भागफल (एचक्यू [HQ]) का अनुमान लगाने के लिए। शेष मानी जाने वाली डंपिंग साइटों की तुलना में नासिक में फ्लार्ड-ऐश डंपिंग साइट मानव स्वास्थ्य के लिए सबसे अधिक खतरा पैदा करने वाली पाई गई। मौखिक अंतर्ग्रहण और त्वचा त्वचीय जोखिम परिदृश्यों के लिए अनुमानित एचक्यू (बच्चे) और एचक्यू (वयस्क) के बीच कोई बड़ा अंतर नहीं देखा गया। विचरण एट्रिब्यूशन विश्लेषण से संकेत मिलता है कि बीडब्ल्यू और ईडी ने बच्चों के लिए अनुमानित एचक्यू की समग्र अनिश्चितताओं में 35% से 55% का योगदान दिया, और

वयस्कों के लिए 95% से अधिक योगदान ईडी द्वारा शासित पाया गया। भारत के कानपुर में क्रोमाइट अयस्क प्रसंस्करण अवशेष (सीओपीआर [COPR]) डंपसाइट्स के कारण पारिस्थितिक और मानव स्वास्थ्य जोखिमों का आकलन करने के लिए एक एकीकृत पारिस्थितिक और एचएचआरए ढांचा विकसित किया गया था। जोखिम मूल्यांकन ढांचे में गतिविधि-विशिष्ट परिदृश्यों के साथ कई जोखिम परिदृश्यों (मौखिक अंतर्ग्रहण और त्वचा त्वचीय संपर्क) और कई मार्गों (मिट्टी और भूजल पथ) पर विचार किया गया था। सभी जनसंख्या समूहों में सभी जोखिम परिदृश्यों के बीच मिट्टी की गतिविधियों में खेलने वाले किशोरों को सबसे अधिक जोखिम वाले क्षेत्र में पाया गया। एचक्यू का औसत मान 4.5 पाया गया, जो सुरक्षित सीमा से चार ऑर्डर अधिक है, और मृदा मार्ग के माध्यम से त्वचा त्वचीय संपर्क जोखिम परिदृश्य के लिए कैंसर जोखिम (सीआर [CR]) का 95वां प्रतिशत मूल्य 9×10^{-4} पाया गया। रानिया साइट के पास भूजल में सुरक्षित सीमा से ऊपर Cr(VI) और U की मौजूदगी, हर जनसंख्या समूह के लिए एक महत्वपूर्ण खतरा पैदा करती पाई गई। सीआर का अधिकतम मूल्य 54.9 पाया गया, जो सभी जनसंख्या समूहों में सबसे अधिक है।

विषम लघु- (30 सेमी) और लंबे-स्तंभ (12.5 मीटर) स्थितियों के माध्यम से विलेय परिवहन को अनुकरण करने के लिए एक उपन्यास शिक्षण शिक्षण-आधारित अनुकूलन (टीएलबीओ [TLBO]) और मोबाइल-इमोबाइल (एमआईएम [MIM]) मॉडल-आधारित एकीकृत दृष्टिकोण लागू किया गया था। एमआईएम मॉडल को 12.5 मीटर लंबे अत्यधिक विषम मृदा स्तंभ में रूढ़िवादी विलेय परिवहन और ग्लेनडेल चिकनी दोमट मिट्टी से भरा हुआ 30 सेमी स्तंभ में प्रतिक्रियाशील विलेय परिवहन के लिए ब्रेकथ्रूकर्व (बीटीसी [BTC]) में विलेय पदार्थ के प्रारंभिक आगमन, चरम सांद्रता और लंबी पूंछ को पकड़ने के लिए पाया गया था। इसके अलावा, संतृप्त छिद्रपूर्ण प्रणाली में बहु-प्रजाति के दूषित पदार्थों के प्रवाह और परिवहन मापदंडों से जुड़ी अनिश्चितता को वैश्विक संवेदनशीलता विश्लेषण (जीएसए [GSA]) का उपयोग करके निर्धारित किया गया था। अस्थायी क्षण-आधारित आउटपुट सूचकांकों के आधार पर दूषित परिवहन मॉडल

के जीएसए ने विभिन्न मॉडल मापदंडों और विभिन्न आउटपुट सूचकांकों पर उनके अलग-अलग प्रभावों के बीच जटिल परस्पर क्रिया का संकेत दिया। इस शोध में 2-डी संख्यात्मक सिमुलेशन से एलपीपीएम क्षेत्रों के साथ और बिना छिद्रित प्रणालियों में देखे गए विपरीत प्लम विकास गतिशीलता पर चर्चा की गई। एलपीपीएम क्षेत्र के साथ छिद्रित प्रणाली में संदूषक द्रव्यमान पुनर्प्राप्ति और औसत निवास समय क्रमशः 25% से 50% कम और 25% से 40% अधिक पाया गया, इसके बिना छिद्रित प्रणाली की तुलना में। अंत में, पीसीई [PCE] और उसके परिवर्तन उत्पादों के रासायनिक मिश्रण के लिए दूषित परिवहन मॉडल-संचालित संभाव्य एचएचआरए का संचालन किया गया। परिवर्तित पुत्री प्रजातियाँ (वीसी [VC], सीआईएस-डीसीई [cis-DCE]) मूल (पीसीई [PCE]) संदूषक प्रजातियों की तुलना में लंबी अवधि (15 वर्ष तक) के लिए मानव स्वास्थ्य के लिए सबसे अधिक खतरा पैदा करती पाई गई। अनुमानित जोखिम मेट्रिक्स में कुल भिन्नता के लिए बीडब्ल्यू, एकाग्रता, ईडी और आईआर को प्रमुख योगदानकर्ता पाया गया। कुल मिलाकर, इस थीसिस में पेश किए गए संभाव्य जोखिम मूल्यांकन दृष्टिकोण और प्रदूषक प्लम गतिशीलता का विश्लेषण करने के तरीके भाग्य और प्रदूषक परिवहन में शामिल जटिलताओं को समझने और नीति निर्माताओं के लिए तकनीकी से गैर-तकनीकी दर्शकों तक ज्ञान को प्रभावी ढंग से स्थानांतरित करने में सहायक हो सकते हैं।

TABLE OF CONTENTS

CERTIFICATE	i
ACKNOWLEDGEMENTS	ii
ABSTRACT	iv
TABLE OF CONTENTS	x
LIST OF FIGURES	xvii
LIST OF TABLES	xxiv
LIST OF ABBREVIATIONS	xxvi
LIST OF MATHEMATICAL NOTATIONS AND SYMBOLS	xxix
CHAPTER ONE	1
INTRODUCTION	1
1.1. Brief Overview.....	2
1.2. Problem Statement.....	5
1.3. Objectives	6
1.4. Scope.....	6
1.5. Dissertation Outline	7
CHAPTER TWO	11
BIBLIOMETRIC ANALYSIS AND LITERATURE REVIEW	11
2.1. General.....	12
2.2. Bibliometric Analysis of Contaminant Transport Modelling in the Groundwater System: Current Trends, Hotspots, and Future Directions	12
2.2.1. Methodology	15
2.2.2. Findings of Bibliometric Analysis of Contaminant Transport Modelling Research Field	19

2.3. Fate and Transport Mechanisms Governing the Multispecies Contaminant Transport in the Porous System.....	32
2.3.1. Effect of Dynamic Groundwater Flow Conditions.....	34
2.3.2. Effect of Mass-transfer Processes between High and Low Permeability Porous Media in the Groundwater System.....	35
2.3.3. Effect of Dissolution.....	36
2.3.4. Effect of Sorption-Desorption in the Aquifer (Mobile) and Aquitard (Immobile) Region.....	37
2.3.5. Effect of Degradation Processes.....	38
2.3.6. Effect of Transverse Dispersion.....	39
2.4. Bibliometric Analysis of DNAPL Transport in the Groundwater System	39
2.4.1. Steps of Bibliometric Analysis	39
2.4.2. Findings of the Bibliometric Analysis of DNAPL Transport Research Field.....	40
2.5. Critical Review on DNAPL Transport in the Groundwater System.....	50
2.5.1. Classification of Studies based on Scale.....	50
2.5.2. Classification of Studies Based on the Type of Modelling Framework Used.....	53
2.6. Mini-Review of Mathematical Modelling Studies related to Indian Context.....	70
2.7. Critical Review on Health Risk Assessment of Subsurface Environment	80
2.7.1. Conventional Health Risk Assessment.....	80
2.7.2. Fate and Contaminant Transport Model-driven Health Risk Assessment.....	83
2.8. Identified Research Questions in the Frame of the Thesis	84
CHAPTER THREE	87
HUMAN HEALTH RISK ASSESSMENT OF GROUNDWATER SYSTEM: MULTI-SCENARIOS-SINGLE-PATHWAY-BASED PROBABILISTIC RISK APPROACH.....	87
3.1. Background.....	88
3.2. Methodology.....	95

3.2.1. Details of the Case Studies	95
3.2.2. Human Health Risk Assessment.....	98
3.2.3. Probabilistic Risk Assessment Framework.....	106
3.2.4. Computation of Spearman’s Rho Statistic.....	106
3.2.5. Variance Attribution Analysis	107
3.3. Results and Discussions.....	107
3.3.1. Statistical Characterization of Hazard Quotients.....	107
3.3.2. Analysis of Inter-relationship between Input Parameters and Estimated Hazard Quotients.....	119
3.3.3. Results of Variance Attribution Analysis	123
3.4. Conclusions.....	126
CHAPTER FOUR.....	127
ECOLOGICAL AND HUMAN HEALTH RISK ASSESSMENT OF SUBSURFACE ENVIRONMENT IN AND AROUND WASTE DUMPSITES: A MULTI-SCENARIOS-MULTI-PATHWAYS BASED PROBABILISTIC RISK APPROACH	127
4.1. Background.....	128
4.2. Methodology.....	131
4.2.1. Study Area and Target Contaminants.....	131
4.2.2. Ecological Risk Assessment.....	134
4.2.3. Human Health Risk Assessment.....	135
4.2.4. Probabilistic Risk Assessment Approach and Uncertainty Quantification.....	141
4.3. Results and Discussion	142
4.3.1. Seasonal Variation of Target Contaminant Concentration in the Groundwater and Soil in the vicinity of Dumpsite	142
4.3.2. Ecological Risk Indexes.....	143
4.3.3. Human Health Risk Assessment for Soil Pathway	147

4.3.4. Human Health Risk Assessment for Groundwater Pathway	150
4.4. Conclusions.....	163
CHAPTER FIVE	165
SOLUTE TRANSPORT MODELLING IN THE HETEROGENEOUS POROUS SYSTEM USING INTEGRATED TEACHING-LEARNING-BASED OPTIMIZATION AND MOBILE-IMMOBILE MODEL.....	165
5.1. Background.....	166
5.2. Methodology	169
5.2.1. Governing Equations of Mobile-Immobile Model	169
5.2.2. Teaching-Learning based Optimization (TLBO) Algorithm.....	171
5.2.3. Execution of Inverse Model, Objective Function and Performance Assessment.....	173
5.3. Results and Discussion	176
5.3.1. Model Verification.....	176
5.3.2. Model Application I: Simulation of Conservative Solute Transport in the Heterogeneous Long Soil Column.....	180
5.3.3. Model Application II: Simulation of Solute Transport through 30 cm Long Column filled Glendale Clay Loam Soil	185
5.4. Conclusions.....	188
CHAPTER SIX	190
ANALYSIS OF MULTISPECIES CONTAMINANT TRANSPORT DYNAMICS IN A SATURATED POROUS SYSTEM USING NUMERICAL SIMULATIONS, TEMPORAL MOMENT, AND GLOBAL SENSITIVITY ANALYSIS.....	190
6.1. Background.....	191
6.2. Methodology	194
6.2.1. Governing Equations of Multispecies Contaminant Transport in the Porous System	195
6.2.2. Sensitivity Analysis Methods	199

6.2.3. Input Parameters and Output Metrics for Global Sensitivity Analysis.....	201
6.3. Verification of Multispecies Contaminant Transport Model.....	203
6.4. Results and Discussion	205
6.4.1. Morris’s method sensitivity indices.....	205
6.4.2. FAST sensitivity indices.....	216
6.4.3. Time-varying global sensitivity analysis	218
6.5. Conclusions.....	223
CHAPTER SEVEN.....	224
UNDERSTANDING THE IMPACT OF LOW PERMEABILITY POROUS MEDIA ON CONTAMINANT PLUME EVOLUTION DYNAMICS USING TWO-DIMENSIONAL NUMERICAL MODELLING AND TEMPORAL MOMENT ANALYSIS	224
7.1. Background.....	225
7.2. Methodology	227
7.2.1. Problem Description and Basic Assumptions.....	227
7.2.2. Governing Equations of Flow and Contaminant Transport.....	228
7.2.3. Temporal Moment Analysis	230
7.2.4. Numerical Modelling Approach	232
7.3. Verification of the Numerical Modelling Approach.....	236
7.4. Results and Discussion	238
7.4.1. Temporal Variation of Contaminant Concentration Distribution for Homogeneous and Heterogeneous Porous System.....	238
7.4.2. Effect of Dispersion Parameters on Contaminant Concentration and Associated Temporal Moments.....	242
7.4.3. Temporal Moments of Reactive Contaminant.....	253
7.5. Conclusion	260
CHAPTER EIGHT.....	262

MULTISPECIES CONTAMINANT TRANSPORT MODEL-DRIVEN PROBABILISTIC HUMAN HEALTH RISK ASSESSMENT OF SUBSURFACE SYSTEM.....	262
8.1. Background.....	263
8.2. Methodology.....	265
8.2.1. Contaminant Transport Model.....	266
8.2.2. Human Health Risk Assessment Model for Multispecies Contaminant.....	272
8.3. Validation of Multispecies Contaminant Transport Model.....	279
8.4. Results and Discussion.....	281
8.4.1. Effect of Longitudinal Dispersion on Concentration Distribution.....	281
8.4.2. Statistical Description of the Human Health Risk Index.....	285
8.4.3. Variance Attribution Analysis of Risk Index.....	288
8.5. Conclusions.....	290
CHAPTER NINE.....	292
CONCLUSIONS AND FUTURE SCOPE.....	292
9.1. Major Conclusions of the Thesis.....	293
9.1.1. Multi-Scenarios-Single-Pathway-based Probabilistic Health Risk Assessment.....	293
9.1.2. Integrated Risk Assessment of Subsurface Environment - Multi-Scenarios-Multi-Pathways-based Probabilistic Risk Approach.....	294
9.1.3. Solute Transport Modelling using Integrated TLBO-MIM Model.....	294
9.1.4. Global Sensitivity Analysis of Multispecies Contaminant Transport Model.....	295
9.1.5. Contaminant Plume Evolution Dynamics in the presence of Low Permeability Porous Media.....	295
9.1.6. Contaminant Transport Model-driven Health Risk Assessment.....	296
9.2. Contributions of the Thesis.....	296
9.2.1. Ecological and Human Health Risk Assessment (Objectives I and II).....	297
9.2.2. Numerical Modelling of Flow and Transport Mechanisms (Objectives III to V)....	297

9.2.3. Mathematical Model-driven Health Risk Assessment (Objective VI)	298
9.3. Limitations of the Thesis	298
9.4. Suggestions for Future Work	299
REFERENCES.....	300
APPENDIX.....	354
LIST OF PUBLICATIONS	403

LIST OF FIGURES

Figure 2. 1 Methodology adopted for bibliometric analysis of CTM research field	16
Figure 2. 2 Variation of publication statistics of CTM with year	20
Figure 2. 3 (a) Country-specific articles production in the CTM, (b) total citations of top-cited country, and (c) average article citation of top-cited country	24
Figure 2. 4 Co-occurrence network of top 20 most influential author's keywords as per Scopus® database from 2010-2022.....	25
Figure 2. 5 Tree plot of top 25 words based on the author's keywords search criteria	27
Figure 2. 6 Co-citation network visualization of authors.....	28
Figure 2. 7 Research cooperation network among authors from different countries obtained from VOSviewer.....	30
Figure 2. 8 Thematic map showing different clusters based on author's keywords	31
Figure 2. 9 A schematic representing the fate and transport of DNAPLs (multispecies contaminants) in the subsurface environment.....	33
Figure 2. 10 Variation of DNAPL transport publication statistics with year	44
Figure 2. 11 Variation of number of publications and cumulative publications with time	45
Figure 2. 12 Country-specific production metrics: (a) number of articles, (b) total citations, and (c) average article citations	47
Figure 2. 13 Spatial distribution of DNAPL contaminated sites in the world along with CPCB designated contaminated sites in India [<i>Data source:</i> (Birke et al. 2003; CPCB 2022; Gupta 2020; USEPA 1999)]	49

Figure 3. 1 (a) Fly-ash dumping site Nashik and Eklahare Thermal Power Plant (Source: Nalawade <i>et al.</i> , 2015 and Google Earth), and (b) Ariyamangalam dumping site (source: Google Earth).....	96
Figure 3. 2 Location of dumping sites in Delhi, India (source: Google Earth)	97
Figure 3. 3 Schematic of the methodology adopted for human health risk assessment	99
Figure 3. 4 Probability distribution of hazard quotient due to Cadmium (Cd) for the adult population group via (a) oral ingestion and (b) skin dermal contact exposure for Ariyamangalam open dumping site.....	109
Figure 3. 5 Average value of hazard quotients (HQ) in the child and adult population groups for oral ingestion and dermal contact exposure scenarios.....	114
Figure 3. 6 Spearman’s rho static computed for cadmium (Cd) at Ariyamangalam open dump	120
Figure 3. 7 Variance contributions of different parameters for Ariyamangalam dumping site via (a) oral ingestion and (b) skin dermal contact exposure scenario	125
Figure 4. 1 Study area with groundwater and soil sampling locations (source: Bhattacharya et al., 2020; Matern et al., 2017).....	132
Figure 4. 2 The framework of ecological and human health risk assessment approach.....	133
Figure 4. 3 Point estimates of geo-accumulation index due to Cr(VI) presence in the soil during pre-monsoon and monsoon season (<i>RP – Rania site – pre-monsoon; KP – Khanchandpur – pre-monsoon; RM– Rania site – monsoon; KM – Khanchandpur - monsoon</i>).....	144
Figure 4. 4 Point estimates of contamination factor due to Cr(VI) presence in the soil during pre-monsoon and monsoon season. (<i>RP – Rania site – pre-monsoon; KP – Khanchandpur – pre-monsoon; RM– Rania site – monsoon; KM – Khanchandpur - monsoon</i>).....	145

Figure 4. 5 Violin plot of probabilistic estimates of **(a)** geo-accumulation index, and **(b)** contamination factor due to Cr(VI) contamination in the soil for pre-monsoon and monsoon season 146

Figure 4. 6 HQ and CR due to the presence of Cr(VI) in the collected soil samples for oral ingestion scenario – soil pathway in the pre-monsoon and monsoon seasons (*95th percentile value*) 148

Figure 4. 7 HQ due to Cr(VI) in the collected soil samples for skin dermal contact scenario – soil pathway in the pre-monsoon and monsoon seasons (*average value from MCS*) 149

Figure 4. 8 Cancer risk (CR) due to Cr (VI) in the collected soil samples for skin dermal contact scenario – soil pathway in the pre-monsoon and monsoon seasons (*average value from MCS*) 150

Figure 4. 9 Box plot of cancer risk (CR) variation due to Cr(VI) for oral ingestion scenario - water pathway 157

Figure 4. 10 Box plot of cancer risk (CR) variation due to Cr(VI) for skin dermal contact scenario - water pathway 159

Figure 5. 1 Flow chart for Teaching–Learning-Based Optimization..... 173

Figure 5. 2 Breakthrough curve predicted by MIM model based upon parameters estimated using TLBO-MIM model for synthetic example..... 177

Figure 5. 3 Variation of objective function with iteration for different runs for case including **(a)** 68 observation points, **(b)** 26 observation points, and **(c)** average of objective function value with iteration for both the cases. 179

Figure 5. 4 Fitting results of MIM numerical solution to the observed BTCs of solute transport in heterogeneous long-soil column obtained from Huang et al. (1995) for **(a)** $x = 100\text{ cm}$, **(b)** $x =$

200 cm, (c) $x = 300$ cm, (d) $x = 350$ cm, (e) $x = 400$ cm, (f) $x = 500$ cm, (g) $x = 600$ cm, (h) $x = 900$ cm, (i) $x = 1000$ cm, and (j) $x = 1200$ cm down-gradient distances 183

Figure 5. 5 Variation of longitudinal dispersivity estimated via TLBO-MIM inverse model with distance for the case of conservative solute transport through 12.5 long-soil column 185

Figure 5. 6 Fitting results of MIM numerical solution to the observed breakthrough curves of solute transport through 30 cm long clay loam soil column (a) linear coordinate system, and (b) logarithmic coordinate system 186

Figure 5. 7 Fitting results of MIM numerical solution to the observed breakthrough curve of reactive solute (Boron) transport for different simultaneous fitting cases 187

Figure 6. 1 Schematic of the methodology used to perform Global Sensitivity Analysis of multispecies contaminant transport model 197

Figure 6. 2 Spatial variations of concentration of species from nitrogen decay chain ($NH_4^+ \rightarrow NO_2^- \rightarrow NO_3^-$) at $t = 200$ hour (Results of present model are shown in solid lines, whereas data from published literature is shown by symbols) 204

Figure 6. 3 Spatial variation of sensitivity index of Morris method for SA output metrics: (a) zeroth temporal moment, (b) first temporal moment, (c) second temporal moment, and (d) coefficient of skewness 209

Figure 6. 4 Ranking of model input parameters estimated using Morris method for SA output metrics: (a) zeroth temporal moment, (b) first temporal moment, (c) second temporal moment, and (d) coefficient of skewness 211

Figure 6. 5 Morris sensitivity results for multispecies reactive transport model for temporal moments: (a) M_0 , (b) T_1 , (c) T_2 , and (d) C_{sk} at $x = 220$ cm down gradient distance 213

Figure 6. 6 Estimates of mean and 95% confidence intervals of mean of EEs from Morris method for various temporal moments computed at $x = 220 \text{ cm}$ downgradient distance	215
Figure 6. 7 Spatial variation of FAST index for (a) zeroth temporal moment ($M0$), (b) first temporal moment ($T1$), (c) second temporal moment ($T2$), and (d) coefficient of skewness (Csk) output metrics.....	217
Figure 6. 8 Time-varying mean of EEs of (a, d) $NH4 +$, (b, e) $NO2 -$, and (c, f) $NO3 -$ species from nitrogen decay chain at 5 cm and 220 cm down-gradient distances	219
Figure 6. 9 Time-varying FAST index for breakthrough curve of (a) $NH4 +$, (b) $NO2 -$, and (c) $NO3 -$ at 5 cm, 100 cm, and 220 cm down-gradient distances	222
Figure 7. 1 Schematic of the mathematical model of saturated porous system with low permeability porous media (LPPM).....	228
Figure 7. 2 Flow chart indicating the workflow for numerical modelling and steps to conduct sensitivity analysis based on temporal moments of concentrations.....	233
Figure 7. 3 Schematic of numerical domain used for verification of modelling approach (<i>based on Verma et al., (2000) and Batu, (1989)</i>).....	237
Figure 7. 4 Variation of normalized concentration with (a) longitudinal and (b) transverse distance at a time, $t = 100$ days	237
Figure 7. 5 Spatial concentration profile of conservative contaminant transport in the porous system (a) without LPPM region and (b) with LPPM region after one year	239
Figure 7. 6 Time evolution of concentration of conservative contaminant at an observation plane positioned at $X = 200 \text{ m}$ (along the longitudinal direction) for (a) porous system without LPPM region and (b) porous system with LPPM region.....	241

Figure 7. 7 Time evolution of distribution of conservative contaminant plume in the porous system without LPPM region for **(a)** $\alpha L = 15 m$, **(b)** $\alpha L = 30 m$, and **(c)** $\alpha L = 60 m$ 244

Figure 7. 8 Time evolution of distribution of conservative contaminant plume in the porous system with LPPM region for **(a)** $\alpha L = 15 m$, **(b)** $\alpha L = 30 m$, and **(c)** $\alpha L = 60 m$ 245

Figure 7. 9 Spatial distribution of temporal moments for different values of longitudinal dispersivity for porous system **(a-c)** without and **(d-f)** with LPPM region 248

Figure 7. 10 Spatial distribution of temporal moments for different values of $\alpha T/\alpha L$ ratio for porous system **(a-c)** without, and **(d-f)** with LPPM region 251

Figure 7. 11 Spatial distribution of **(a, b)** solute mass recovery, and **(c, d)** mean residence time for porous system **(a, c)** without and **(b, d)** with LPPM region. *The retardation factor varied as $R = 1, 2$, and 4 . A line with a squared symbol represents $R = 1$, whereas a line with a triangle symbol represents $R = 4$.*..... 254

Figure 7. 12 Spatial distribution of variance of BTC for porous system **(a)** without and **(b)** with LPPM region with different values of retardation factor. *The retardation factor varied as $R = 1, 2$, and 4 . A line with a squared symbol represents $R = 1$, whereas a line with a triangle symbol represents $R = 4$.*..... 256

Figure 7. 13 Spatial distribution of **(a, d)** zeroth temporal moment, **(b, e)** mean residence time, and **(c, f)** variance of BTC for different values of head gradients for porous system **(a-c)** without, and **(d-f)** with LPPM region 259

Figure 8. 1 Framework of fate and contaminant transport model-driven probabilistic human health risk assessment approach 266

Figure 8. 2 Schematic showing fate and contaminant transport modelling approach 268

Figure 8. 3 Spatial variations of contaminant concentration (C_1, C_2, C_3) at time (t) = 400 hour	280
Figure 8. 4 Probability distribution of concentration at various time levels: (a) 1 st year, (b) 5 th year, (c) 10 th year, and (d) 50 th year.....	282
Figure 8. 5 Mean value of concentration of parent and daughter contaminant species at $xL =$ 500 m with maximum concentration level (MCL)	283
Figure 8. 6 Concentration distribution of parent and daughter contaminant species with time	284
Figure 8. 7 Temporal variation of the mean value of (a) total non-carcinogenic index and (b) total carcinogenic health risk index	286
Figure 8. 8 The 95 th percentile value of non-carcinogenic risk index due to individual contaminant species for a child population group	287
Figure 8. 9 The 95 th percentile value of non-carcinogenic risk index due to individual contaminant species for an adult population group	288
Figure 8. 10 Variance contributions of different parameters for carcinogenic risk estimates at 5 th year.....	289

LIST OF TABLES

Table 2. 1 Steps used for data collection from the Scopus [®] database.....	17
Table 2. 2 Steps followed for data collection.....	41
Table 2. 3 Main descriptions of DNAPL transport review Scopus [®] database.....	43
Table 2. 4 List of Most Influential Authors in the Research Field based on <i>NoA</i> main criteria..	46
Table 2. 5 Source Mass Release Models used in the studies pertaining to dissolved DNAPL....	54
Table 2. 6 Mathematical modelling-based studies emphasizing fate and transport of DNAPLs.	62
Table 2. 7 Summary of mathematical modelling-based studies (Indian context).....	72
Table 3. 1 Environmental risk assessment-based studies conducted in the Indian regime	90
Table 3. 2 Description of data collected from various dumping sites in India	100
Table 3. 3 Values of detected metal concentration used in risk estimation	100
Table 3. 4 Input parameters used in risk estimation.....	103
Table 3. 5 Permeability coefficient of metal in water	104
Table 3. 6 Values of reference dose [mg/kg-day] (<i>Source: USDOE, 2010*</i> ; <i>USEPA, 2016[#]</i>).	105
Table 3. 7 Statistical characterization of HQ for Okhla dumping site based on data from Ram et al. (2016).....	110
Table 3. 8 Comparison of dumping sites/landfills based on the average values of hazard quotient	117
Table 3. 9 Spearman’s rho statistic calculated for Ariyamangalam open dumping site	121
Table 4. 1 Classes of the geoaccumulation index	134
Table 4. 2 Classes of the contamination factor	134
Table 4. 3 Summary of exposure model parameters.....	139

Table 4. 4 Contaminants specific values for various parameters used in risk estimation.....	141
Table 4. 5 Statistical characterizations of HQ posed by Rania COPR dump site for oral ingestion exposure scenario during pre-monsoon season.....	151
Table 4. 6 Statistical characterizations of HQ posed by Rania COPR dump site for skin dermal contact exposure scenario during pre-monsoon season	152
Table 4. 7 Statistical characterizations of HQ posed by Rania COPR dump site for oral ingestion exposure scenario during monsoon season.....	154
Table 4. 8 Statistical characterizations of HQ posed by Rania COPR dump site for skin dermal contact exposure scenario during monsoon season	155
Table 5. 1 Estimated parameters of MIM model and associated performance indicators at different distances of a heterogeneous soil column.....	184
Table 5. 2 Estimated parameters of MIM model and associated performance assessment indicators for solute transport through 30 cm long column-filled Glendale clay loam soil.....	188
Table 6. 1 Input parameters used for model verification	203
Table 6. 2 Parameters of multispecies contaminant transport model and associated uncertainty range.....	206
Table 7. 1 Input parameters used for numerical simulations	234
Table 8. 1 Input parameters used in the fate and contaminant transport model.....	270
Table 8. 2 Input parameters related to dermal contact risk calculations	274
Table 8. 3 Values of reference dose, slope factor, and MCL for various DNAPL compounds.	277
Table 8. 4 Input model parameters of HHRA	278
Table 8. 5 Input parameters used for validation of multispecies contaminant transport model	280

LIST OF ABBREVIATIONS

1-D	One dimensional	MADE	Macro-dispersion experiment
2-D	Two dimensional	MC	Monte Carlo
2RNE	Two-region non-equilibrium	MCL	Maximum concentration level
3-D	Three dimensional	MCS	Monte Carlo simulations
AACi	Average article citation	MIM	Mobile-immobile
ADE	Advection dispersion equation	MNW	Multi-node well
AF	Adherence factor	MODFLOW	Modular Three-Dimensional Finite-Difference Groundwater Flow Model
AT	Averaging time	MPNE	Multi processes non equilibrium
BA	Bees Algorithm	MRMT	Multi-rate mass transfer
BTC	Breakthrough curve	MRT	Mean residence time
BTEX	Benzene, Toluene, Ethylbenzene, Xylene	MSW	Municipal solid waste
BW	Body weight	MT3DMS	Modular Three-dimensional Multispecies Transport Model for Simulation
CDI	Chronic daily intake	MTBE	Methyl tert-butyl ether
CF	Contamination factor	MTC	Mass transfer correlations
CI	Confidence interval	NoA	Number of articles
Cis-DCE	cis-Dichloroethene	NSE	Nash-Sutcliffe efficiency
COM	Center of mass	NTPP	Nashik Thermal Power Plant
COPR	Chromite ore processing residue	OpenFOAM	Open-source Field Operation And Manipulation
CPCB	Central pollution control board	PCE	Tetrachloroethene

CR	Cancer risk	PHT3D	Three-dimensional Reactive Multicomponent Transport Model for Saturated Porous Media
CTM	Contaminant transport modelling	PRA	Probabilistic risk assessment
CTRW	Continuous time random walk	PRF	Probabilistic risk framework
DAD	Dermally absorbed dose	PRZM	Pesticide root zone model
DNAPL	Dense non-aqueous phase liquid	PSO	Particle Swarm Optimization
DRA	Dose-response assessment	PSY	Publication year
DYNIA	Dynamic identification analysis	RfD	Reference dose
ECC	Estarreja chemical complex	RMSE	Root mean square error
ED	Exposure duration	RPCM	Radial point collocation method
EE	Elementary effect	RSA	Regional sensitivity analysis
EF	Exposure frequency	RT3D	Reaction transport code
EV	Event frequency	RWhet	Random-walk based method
FAST	Fourier Amplitude Sensitivity Test	RWPT	Random walk particle tracking
FDM	Finite difference method	SA	Skin surface area
FEFLOW	Finite Element subsurface FLOW system	SAFE	Sensitivity Analysis For Everyone
FEM	Finite element method	SF	Slope factor
GCW	Groundwater circulation well system	SRCC	Spearman's rank correlation coefficient

GLUE	Generalized likelihood uncertainty estimation	SUTRA	Saturated-unsaturated transport
GMS	Groundwater modelling system	TBA	Tert-butyl alcohol
GSA	Global sensitivity analysis	TCA	Tetrachloroethane
GWS	Groundwater system	TCE	Trichloroethene
HHRA	Human health risk assessment	TCi	Total number of citations
HI	Hazard index	TDS	Total dissolved solid
HQ	Hazard quotient	TIAA	Tucson International Airport Area
ICET ³	Integrated contaminant elution and tracer test toolkit	TLBO	Teaching-Learning Based Optimization
IFRC	Integrated Field Research Challenge	T-PROGS	Transition Probability Geostatistical Software
IR	Ingestion rate	USDOE	U.S. Department of Energy
IRIS	Integrated Risk Information System	USEPA	United States Environmental Protection Agency
IWAM	Integrated water resource assessment and modelling	VAFB	Vandenberg Air Force Base
KGE	Kling Gupta Efficiency	VC	Vinyl chloride
LPPM	Low permeability porous media	ZTM	Zeroth temporal moment

LIST OF MATHEMATICAL NOTATIONS AND SYMBOLS

\overline{C}^{model}	Mean of model simulated concentration	λ_i	First-order degradation coefficient of i^{th} species
$\overline{C}^{observed}$	Mean of observed concentration	μ_i	Mean of the elementary effects
C_{soil_i}	Concentration of target contaminant in soil sample	μ_{lim}	First-order dissolved-phase decay coefficient immobile region
K_{dim}	Sorption distribution coefficient in the immobile region	μ_{lm}	First-order dissolved-phase decay coefficient in mobile region
K_{dm}	Sorption distribution coefficient in the mobile region	μ_n	Normalized temporal moment of n^{th} order
A_i	i^{th} input variable with variance ($Var(A_i)$)	μ_{sim}	First-order sorbed-phase decay coefficient in immobile region
B_n	Metal background/reference concentration	μ_{sm}	First-order sorbed-phase decay coefficient in mobile region
C_0	Injected concentration of solute source	ρ_b	Bulk density of the porous medium
C_i	Concentration of target contaminant in leachate or groundwater	σ_i	Standard deviation of elementary effects
C_{im}	Concentrations in the immobile region	σ_{model}	Standard deviation of model simulated concentration
C_i^{model}	i^{th} model simulated concentration	$\sigma_{observed}$	Standard deviation of observed concentration

$C_i^{observed}$	i^{th} observed concentration	τ_L	Tortuosity factor
C_m	Concentrations in the mobile region	ϵ_p	Liquid volume fraction
C_s	Metal concentration in soil	Δt	Time step
$C_{sk}(x)$	Coefficient of skewness at location x	Δx	Mesh size
$D_{L,i}$	Molecular diffusion coefficient of species diluted in pure liquid	∇p	Pressure difference between inlet and outlet of domain
$D_{e,i}$	Effective diffusion coefficient in saturated porous media	ABS_{GI}	Dimensionless fraction of absorbed contaminant in the gastrointestinal tract
$D_{m,i}$	Molecular diffusion coefficient of i^{th} species in water	ABS	Dimensionless fraction of absorbed contaminant
I_{geo}	Geo-accumulation index	$ADD_i(GW)$	Chronic daily intake for groundwater pathway
J_i	Mass flux vector	$ADD_i(soil)$	Chronic daily intake for soil pathway
$K_{d,i}$	Sorption distribution coefficient of i^{th} species	CV_{model}	Coefficient of variation of model simulated concentration
L_x	Dimension of domain along x -direction	$CV_{observed}$	Coefficient of variation of observed concentration
L_y	Dimension of domain along y -direction	CF	Contamination factor
$M_0(x)$	Zeroth temporal moment at location x	CSF_{ABS}	Cancer slope factor for skin dermal contact
M_i	Mean of solutions	CSF_O	Cancer slope factor for oral ingestion

M_n	n^{th} order absolute temporal moment	CSF	Cancer slope factor
Q_m	Mass source term	D	Hydrodynamic dispersion coefficient
R^2	Determination coefficient	DA_{event_i}	Absorbed dose per event for groundwater pathway
R_i	Retardation factor of i^{th} species	DA_{event}	Absorbed dose per event
$T_1(x)$	Mean residence time at location x	$DAD_i(GW)$	Dermally absorbed dose for groundwater pathway
$T_2(x)$	Variance of breakthrough at location x	$DAD_i(soil)$	Dermally absorbed dose for soil pathway
T_F	Teaching factor	FA	Fraction of skin in contact with water
T_i	Teacher at i^{th} iteration	IR_{soil}	Soil ingestion rate
$X_{new,i}$	New solution	K	Hydraulic conductivity
$X_{old,i}$	Old solution	L	Total length of numerical domain
$d_i(j)$	Elementary effect determined for i^{th} parameter by using j^{th} sampling point	N	Number of observation points
e_i	Difference between simulated and observed concentrations	OF	Objective function
f_{A_i}	Variance contribution of A_i to the overall variance of the estimated risk index	RfD_{ABS}	Reference dose for absorption
f_A	Variance contribution of A to the overall variance of the estimated hazard quotient	RfD_O	Reference dose for oral ingestion exposure scenario

k_p	Dermal coefficient of permeability of contaminant	RfD	Reference dose
r_i	Random number	SA_{soil}	Skin surface area for soil pathway
t^*	Time to reach a steady-state for DNAPL	$Var(HQ)$	Variance of estimated hazard quotient
t_{event}	Single contact event duration	$Var(RI)$	Variance of estimated risk index
t_{pulse}	Pulse duration	Y	Yield coefficient for transformation from one to another species
v_m	Porewater velocity in the mobile region	f	Fractions of sorption sites that equilibrate rapidly with the mobile region
y_i	Effective yield coefficient for any reactant or product pair representing the mass ratio of species (i) produced to the species ($i - 1$) consumed	q	Flowrate
$\alpha_{L,c}$	Dispersivity along longitudinal direction	t	Time
α_L	Longitudinal dispersivity	u	Darcy velocity
$\alpha_{T,c}$	Dispersivity along transverse direction	v	Porewater velocity
α_{TH}	Horizontal transverse dispersivity	$weight_i$	Normalized weight coefficient
α_{long}	Longitudinal dispersivity	x	Spatial coordinate
β_{bias}	Bias ratio	β	Ratio of mobile region to total pore volume

$\gamma_{variability}$	Variability ratio	θ	Total volumetric water content
θ_{im}	Volumetric water content of immobile region	ρ [risk assessment]	Spearman's rho statistic
θ_m	Volumetric water content of mobile region	ω	First-order mass transfer coefficient